

# Structural and functional characterization of the interaction between the influenza A virus RNA polymerase and the CTD of host RNA polymerase II

Jeremy Keown,<sup>1</sup> Alaa Baazaoui,<sup>2</sup> Marek Šebesta,<sup>3</sup> Richard Štefl,<sup>3,4</sup> Loïc Carrique,<sup>1</sup> Ervin Fodor,<sup>2</sup> Jonathan M. Grimes<sup>1</sup>

**AUTHOR AFFILIATIONS** See affiliation list on p. 12.

**ABSTRACT** Influenza A viruses, causing seasonal epidemics and occasional pandemics, rely on interactions with host proteins for their RNA genome transcription and replication. The viral RNA polymerase utilizes host RNA polymerase II (Pol II) and interacts with the serine 5 phosphorylated (pS5) C-terminal domain (CTD) of Pol II to initiate transcription. Our study, using single-particle electron cryomicroscopy (cryo-EM), reveals the structure of the 1918 pandemic influenza A virus polymerase bound to a synthetic pS5 CTD peptide composed of four heptad repeats mimicking the 52 heptad repeat mammalian Pol II CTD. The structure shows that the CTD peptide binds at the C-terminal domain of the PA viral polymerase subunit (PA-C) and reveals a previously unobserved position of the 627 domain of the PB2 subunit near the CTD. We identify crucial residues of the CTD peptide that mediate interactions with positively charged cavities on PA-C, explaining the preference of the viral polymerase for pS5 CTD. Functional analysis of mutants targeting the CTD-binding site within PA-C reveals reduced transcriptional function or defects in replication, highlighting the multifunctional role of PA-C in viral RNA synthesis. Our study provides insights into the structural and functional aspects of the influenza virus polymerase-host Pol II interaction and identifies a target for antiviral development.

**IMPORTANCE** Understanding the intricate interactions between influenza A viruses and host proteins is crucial for developing targeted antiviral strategies. This study employs advanced imaging techniques to uncover the structural nuances of the 1918 pandemic influenza A virus polymerase bound to a specific host protein, shedding light on the vital process of viral RNA synthesis. The study identifies key amino acid residues in the influenza polymerase involved in binding host polymerase II (Pol II) and highlights their role in both viral transcription and genome replication. These findings not only deepen our understanding of the influenza virus life cycle but also pinpoint a potential target for antiviral development. By elucidating the structural and functional aspects of the influenza virus polymerase-host Pol II interaction, this research provides a foundation for designing interventions to disrupt viral replication and transcription, offering promising avenues for future antiviral therapies.

**KEYWORDS** influenza, RNA polymerases, transcription, RNA polymerase II, CTD

Influenza viruses are negative-strand RNA viruses with a genome consisting of eight viral RNA (vRNA) segments organized into viral ribonucleoprotein (vRNP) complexes (1). Each vRNP complex packages one viral genome segment using viral nucleoprotein (NP) and viral RNA-dependent RNA polymerase (RdRp), a heterotrimeric protein, that consists of the polymerase acidic (PA), polymerase basic 1 (PB1), and PB2 subunits (2). During viral infection, the vRNPs are trafficked to the cell nucleus where the viral

**Editor** Anice C. Lowen, Emory University School of Medicine, Atlanta, Georgia, USA

Address correspondence to Ervin Fodor, [ervin.fodor@path.ox.ac.uk](mailto:ervin.fodor@path.ox.ac.uk), or Jonathan M. Grimes, [jonathan.grimes@strubi.ox.ac.uk](mailto:jonathan.grimes@strubi.ox.ac.uk).

Jeremy Keown and Alaa Baazaoui contributed equally to this article. Author order was determined on the basis of seniority.

The authors declare no conflict of interest.

See the funding table on p. 13.

**Received** 19 January 2024

**Accepted** 10 March 2024

**Published** 2 April 2024

Copyright © 2024 Keown et al. This is an open-access article distributed under the terms of the [Creative Commons Attribution 4.0 International license](https://creativecommons.org/licenses/by/4.0/).

polymerase performs both viral transcription and replication. Replication, a two-step process, is primer independent and requires *de novo* initiation by the viral polymerase to synthesize new vRNA, using positive-sense complementary RNA (cRNA) as an intermediate template (2, 3). In contrast, viral transcription depends on the interaction of the viral polymerase with the host transcriptional machinery to produce viral positive-sense mRNA. The synthesized viral mRNA contains a 5′ terminal N7-methyl guanosine (m7G) cap and a 3′ polyA tail which makes viral mRNA structurally identical to the host mRNA and allows the virus to hijack the host translation machinery for viral protein synthesis in the cytoplasm (2, 4). In a process called “cap snatching”, the viral polymerase steals 10–15 nucleotides long capped RNA fragments from nascent capped host RNA, generated by the host RNA polymerase II (Pol II), to prime its own transcription using the PB2 cap-binding and PA endonuclease domains (4, 5). Cap snatching takes place during the early stages of Pol II-mediated transcription which enables the viral polymerase to secure access to host RNA caps before being bound by host cap-binding proteins (6). The interaction of the viral polymerase with Pol II has detrimental effects on host transcription and results in inhibition of cellular gene expression (host shut-off) and Pol II degradation at later stages of infection (7–9).

To access caps of nascent host RNA, the viral polymerase physically associates with host Pol II. Functional and structural studies confirmed that the viral polymerase selectively recognizes the serine 5 phosphorylated (pS5) CTD heptad repeat sequence YSPTpSPS, the signature for initiating Pol II involved in capping (4, 10). In structural studies, two distinct binding sites of the CTD to the viral polymerase were observed using polymerase from influenza virus types A, B, and C and synthetic four-repeat pS5 CTD peptides (11–13). Structures of the CTD-bound polymerase of different influenza types revealed shared and distinct binding features between each type, while binding of the Pol II CTD beyond the identified binding sites remains largely unknown. Considering that mammalian Pol II CTD contains 52 heptad repeats of the consensus sequence Y<sub>1</sub>S<sub>2</sub>P<sub>3</sub>T<sub>4</sub>S<sub>5</sub>P<sub>6</sub>S<sub>7</sub>, which far exceeds the length of CTD mimetic peptides, it appears likely that further interactions between the viral polymerase and Pol II CTD take place beyond the identified binding sites (4, 10). In addition, it has been reported that the interaction of the viral polymerase with Pol II involves not only the CTD of the large subunit, RPB1, but also other subunits of the 12-subunit holoenzyme such as RPB4 (11, 14).

Here, we present the structures of the CTD-bound polymerase of the 1918 pandemic influenza A virus. In these structures, we observe a continuous stretch of the CTD binding site, encompassing 25 of the 28 amino acid residues of the four heptad repeats (repeats a–d), on the C-terminal domain of the PA subunit (PA-C). Additionally, we observe a minor population of particles with a unique arrangement of the PB2 C-terminal (PB2-C) region, likely representing a transcriptase intermediate. Based on these structures, we performed mutagenesis of residues in the CTD-binding site that are conserved across influenza A virus strains, with the aim of determining their effect on viral polymerase activity using a cell-based vRNP reconstitution assay. Our findings demonstrate that mutagenesis of conserved residues in the CTD binding site results in transcriptional and replicational defects, indicating a potential overlap of binding sites for host factors that facilitate transcription and replication, respectively.

## RESULTS

### Effect of alternative phosphorylation patterns of the Pol II CTD on binding the influenza A virus polymerase

The Pol II CTD exhibits remarkable functional flexibility because many of the amino acids in the heptapeptide can undergo posttranslational modifications, and various combinations of these covalent marks are selectively recognized by different protein partners (15–18). Of the amino acid residues composing the consensus heptad, serines at positions 2, 5, and 7 (abbreviated as S2, S5, and S7, respectively) as well as the tyrosine at position 1 (Y1) and the threonine at position 4 (T4) can be phosphorylated. Mass spectrometry analysis revealed that S2 and S5 phosphorylations are the most

prominent posttranslational modifications (19, 20). More recently, several studies linked S7 phosphorylation to early events of transcription initiation (21). The influenza virus polymerase has been shown to have a strong preference for the pS5 CTD over pS2 and unphosphorylated CTD (22). However, combinations of these main phosphorylation patterns and the effect of pS7 have not yet been investigated.

To further characterize the binding preference of the influenza virus polymerase to Pol II CTD, we used biotinylated Pol II CTD mimic peptides containing four repeats (designated repeats a–d) of the conserved heptapeptide repeat (Y<sub>1</sub>S<sub>2</sub>P<sub>3</sub>T<sub>4</sub>S<sub>5</sub>P<sub>6</sub>S<sub>7</sub>) with a combination of phosphorylation patterns (Fig. 1; Fig. S1; Table S1). We opted for peptides with four heptapeptide repeats as it has been demonstrated previously that these can bind the influenza virus polymerase specifically (13, 22). We found that the polymerase of the 1918 pandemic influenza virus bound to the pS5 peptide, and we also detected low but above background levels of binding to pS7. Interestingly, none of the other peptides were bound by the viral polymerase above background. Overall, this experiment shows that the influenza virus polymerase has a striking preference for pS5 peptide compared to pS2 and pS7 and additional phosphorylation in the pS5 peptide interferes with binding. This binding preference clearly links the influenza virus polymerase to the initiating form of Pol II engaged in capping its nascent RNA (23).

### Structure of the 1918 pandemic influenza A virus polymerase bound to Pol II CTD mimic peptide

To characterize the binding of the CTD of host Pol II to the 1918 pandemic influenza A virus polymerase, we used recombinant influenza virus polymerase expressed in insect cells and a four-repeat synthetic pS5 Pol II CTD mimic peptide. Cryo-EM analysis of the complex generated a high-quality map to a global resolution of 3.22 Å (Fig. 2A; Fig. S2) comprising the polymerase core (PA-C, PB1, PB2-N domains), the PA endonuclease domain, 15 bases of the 5′ vRNA promoter, 8 bases from the 5′ end of the 3′ vRNA promoter, and continuous density for 25 amino acids of the CTD peptide (Fig. 2B). Though capped RNA was added to the complex, this was not observed either in the RdRp active site or in the PB2 cap-binding domain. The PB2-C domains were not observed in the consensus refinement.

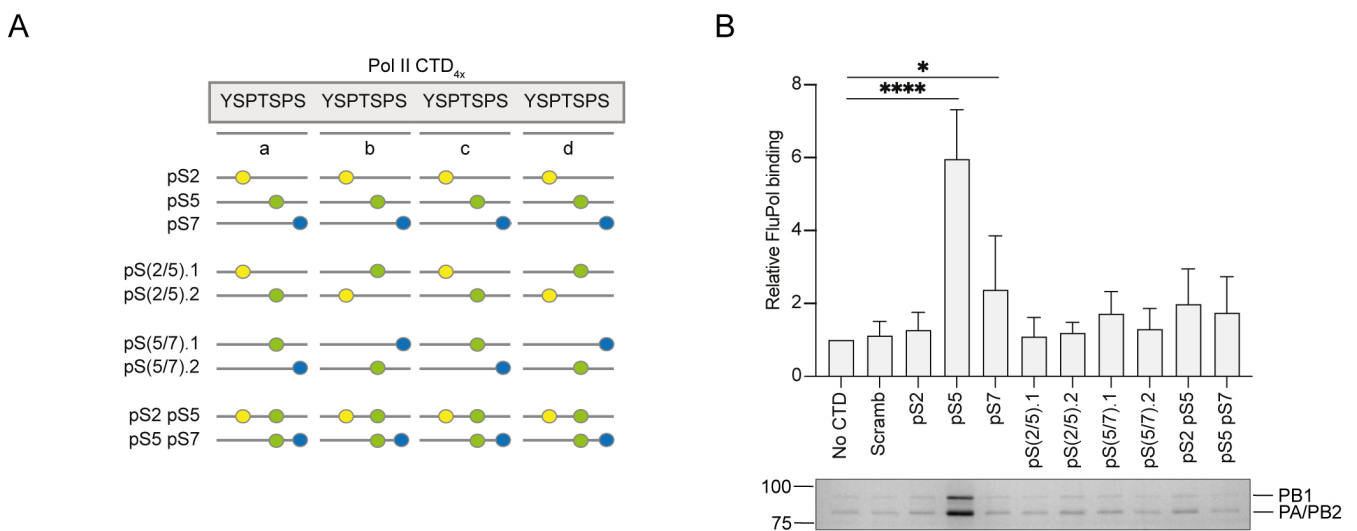


**FIG 1** Effect of serine phosphorylations of Pol II CTD on binding the 1918 pandemic H1N1 influenza A virus polymerase. (A) Schematic of peptides used in the binding assay with the four heptapeptide repeats (designated repeats a, b, c, and d) depicted as gray lines. Serine phosphorylations (pS) are shown as colored circles [pS2 (yellow), pS5 (green), pS7 (blue)]. (B) Binding of the influenza virus polymerase to serine phosphorylated Pol II CTD mimic peptides. Top panel, quantification of influenza virus polymerase (FluPol) binding from  $n = 3$  independent binding assays. Data are mean  $\pm$  SEM. Ordinary one-way ANOVA was used to compare the relative polymerase binding in the presence and absence of CTD. \* $P < 0.05$ ; \*\*\*\* $P < 0.0001$ . Bottom panel, a representative silver-stained gel.

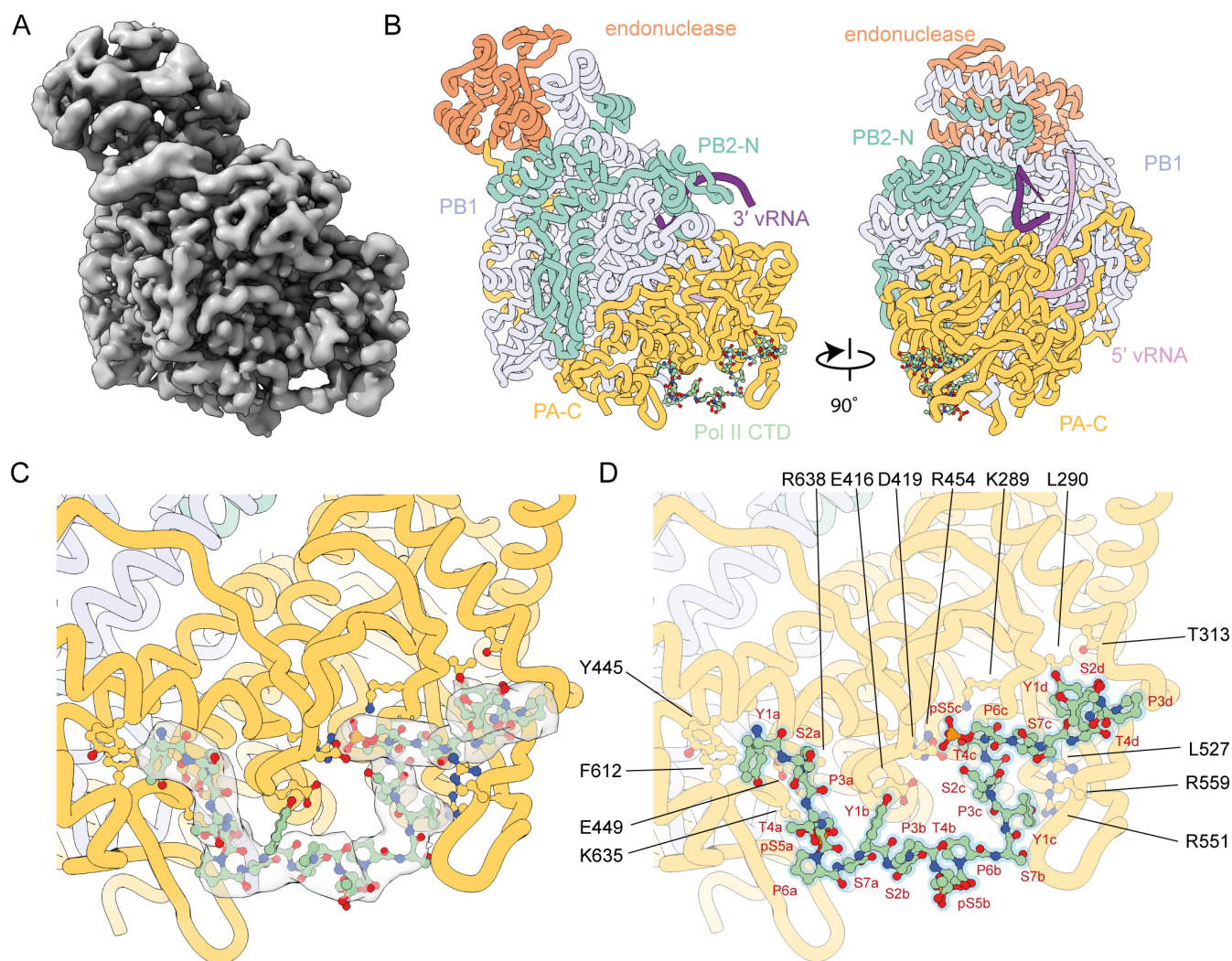


**FIG 2** Structure of the 1918 pandemic H1N1 influenza A virus polymerase bound to a pS5 Pol II CTD mimic peptide. (A and B) deepEMhancer modified cryo-EM map (A) and model in two orientations showing the position of the CTD peptide bound at PA-C domain (B). (C and D) Close-up views detailing the interaction of the CTD peptide with the PA-C domain showing the fit of the peptide model (C) and amino acids involved in mediating the interactions (D).

The global polymerase conformation is that of a transcriptase as characterized by the position of the endonuclease domain packing against the PB1 C-terminal helices (24–26). The CTD occupies an elongated binding site along the PA-C domain, where we observe 25 of the 28 residues from the peptide (Fig. 2C). The phosphorylated peptide buries a total surface area of 1,160 Å<sup>2</sup> with the interaction mediated predominantly by the first (designated repeat a), third (designated repeat c), and the N-terminal half of the fourth heptad repeat (designated repeat d). The phosphorylated serine residues pS5a and pS5c of the peptide are highly ordered and are coordinated into binding sites formed by K635/R638 and K289/R454, respectively. E416 and E457 aid in the correct positioning of R454 to coordinate pS5c. Other amino acid residues of the polymerase interact with unmodified residues from the CTD peptide. Specifically, residues Y445, E449, and F612 interact with Y1a and D419 may contact Y1b. At the C-terminal end of the resolved part of the peptide L290 and Y313 contact Y1d, L527 may interact with P6c, and R551/R559 contact the peptide as it leaves the surface of the PA-C over the top of the PA 550-loop. The phosphorylated pS5b was partially ordered showing a clear main chain and does not appear to contact the polymerase core (Fig. 2D). All residues interacting with the peptide are from the PA subunit. The observed CTD binding site is similar to that

observed previously for other influenza A virus polymerases as well as influenza B and C virus polymerases, underpinning the conserved role of PA-C in binding Pol II CTD (Fig. S3). However, there are clear distinctions in the mode of CTD binding involving different regions of PA-C for the polymerases of the three different influenza types. Additionally, in contrast to influenza A, in influenza B, the CTD binding site extends to the PB2 627-NLS domain, while in influenza C polymerase, the binding site also involves amino acid residues from the PB1 subunit. Together, these data show that although polymerases of all three influenza types use PA-C as the main interface for Pol II CTD binding, the mode of binding has diverged between influenza virus types involving distinct regions.

### Arrangement of PB2-C in the Pol II CTD-bound influenza virus polymerase

While most particles in our cryo-EM data set lacked density for the flexible PB2-C domains, including the cap-binding domain, mid-link, 627, and nuclear localization signal (NLS) domains, approximately 5% of the particles from the consensus refinement contained additional electron density, suggesting that in these particles the PB2-C domains had become ordered (Fig. 3A; Fig. S2). By aligning the core of previously determined polymerase structures, we were able to accurately position the cap-binding domain and mid-link domain in the density (Fig. 3B). The position of these two domains was essentially identical to that of the recently determined transcription intermediate structure (PDB ID 7NHX) (27). In this model, the mid-link domain has remained in close contact with the core of the polymerase (in a position common to transcriptase conformations), while the cap-binding domain has retracted away from the core and primer entry channel. A putative role of this conformation was recently proposed, as an intermediate state between transcription and replication (28). To aid our attempts to unambiguously orient the 627 domain and/or the NLS, we utilized deepEMhancer to modify the map. From this modified map, we could unambiguously position the 627 domain such that the connectivity to the mid-link was maintained and with a good fit to the modified density (Fig. S4).

The 627 domain and NLS in this model adopt a position that is distinct from their location in either a replicating polymerase, encapsidating polymerase, or previously observed transcription initiation or cap-snatching structures (Fig. 3C) (29). In this model, the 627 domain and NLS have rotated 155° and moved 27 Å from the transcription initiation position (Fig. 3D). The movement changes the interaction with the polymerase from contacting the PA and PB1 subunits through a three stranded beta-sheet formed by residues 640–676 such that it now contacts the PA-C and PB2-N2 domains through residues 643–654. This interface is smaller than observed in the transcription initiation conformation resulting in this domain being poorly resolved. A small interface was formed between the NLS and residues from the PB1 (583–587), PB2 (125–127), and PA (430–432) subunits. Although we can precisely position the protein domains, due to the low resolution, we were unable to accurately describe residue contacts in these regions. This relocation of the 627 domain and NLS brings them proximal to the N-terminus of the Pol II CTD peptide, but we do not observe any additional peptide density for Pol II CTD in this reconstruction that would suggest a direct contact between the CTD and the PB2-C. However, given the low-resolution maps, we cannot exclude the possibility of a direct contact. In fact, electrostatic analysis of the surface of the 627 domain that is oriented toward the N-terminus of the CTD peptide shows a highly basic surface (Fig. 3E). This surface would likely be able to bind the negatively charged phosphorylated CTD peptide. Recent structural evidence of Pol II CTD binding to the influenza B virus polymerase demonstrates a large additional CTD-binding site across the surface of the 627 domain (11, 13). In line with this, deletion of the 627 domain from the influenza B virus polymerase dramatically reduced binding to Pol II CTD, while a similar deletion did not affect the ability of the influenza A virus polymerase to bind CTD (11). It is possible that the loss of binding from the deletion of the 627

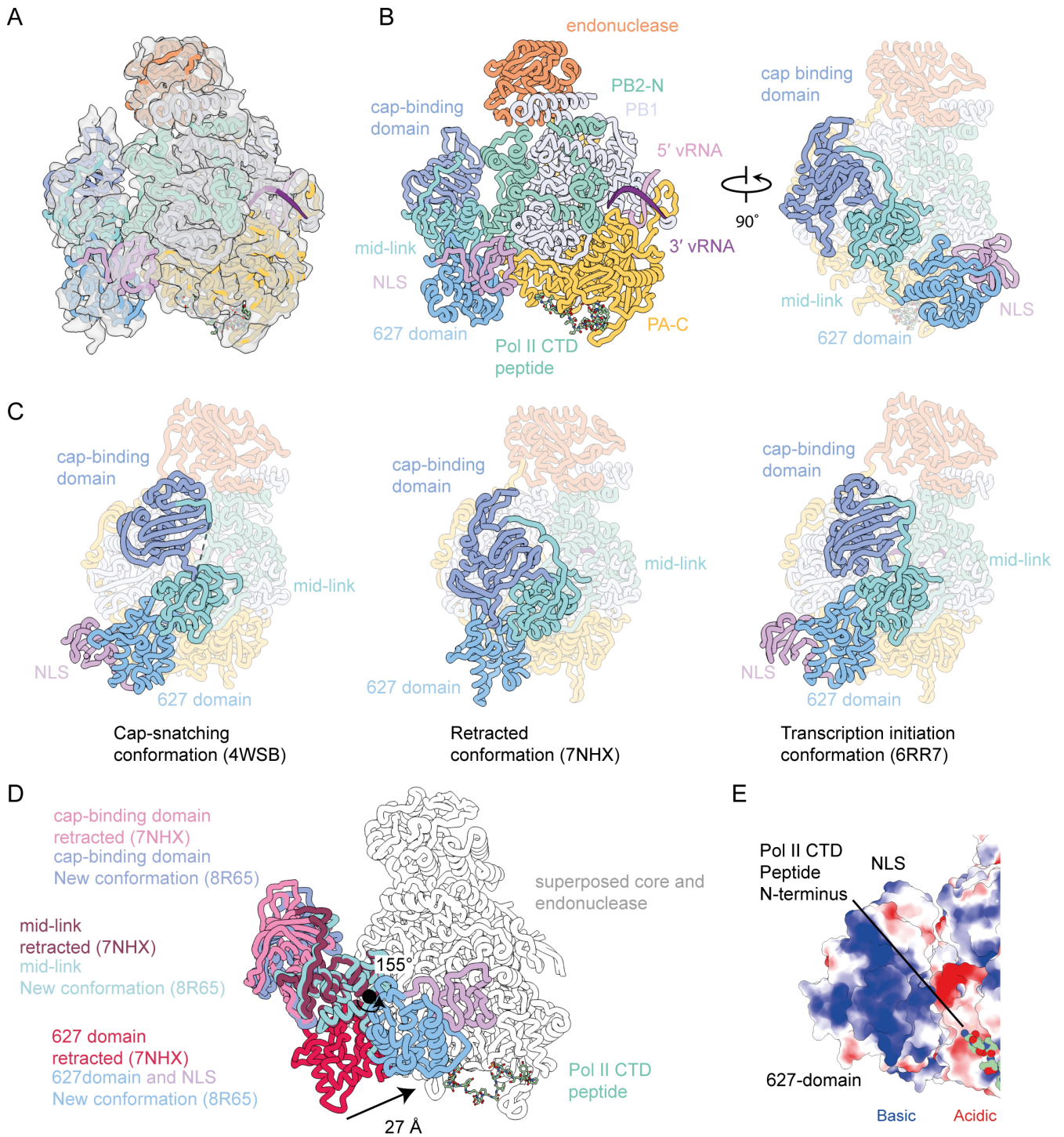


**FIG 3** Structure of the 1918 pandemic H1N1 influenza A virus polymerase bound to a p55 Pol II CTD mimic peptide with resolved PB2-C domains. (A and B) deepEMhancer modified cryo-EM map (A) and model in two orientations showing the domain structure with the arrangement of the PB2-C domains highlighted on the right (B). (C) Previously determined structures of the influenza virus polymerase with different arrangements of the PB2-C domains highlighted. (D) Structures of the 1918 CTD-bound polymerase and the polymerase in the retracted conformation superposed on the polymerase core and endonuclease domain (shown in gray). The PB2-C domains are highlighted in different colors, and the 27 Å movement of the PB2 627 domain is indicated. (E) Electrostatic analysis of the PB2 627 domain that is oriented toward the N-terminus of the CTD peptide shows a highly basic surface.

domain is compensated by the larger binding surface of the CTD peptide on the influenza A virus PA-C domain.

## Effect of mutations in the PA-C Pol II CTD binding site on polymerase function

To address the role of the identified Pol II CTD-binding site in PA-C in polymerase function, we used a vRNP reconstitution assay followed by the analysis of RNA by primer extension. We co-expressed the three polymerase subunits, nucleoprotein, and segment 6 encoding the neuraminidase vRNA in HEK 293T cells to assemble vRNPs, the minimal viral complex required for transcription (mRNA synthesis), and genome replication (cRNA and vRNA synthesis) (Fig. S5). Based on our structural model and previously determined polymerase structures from influenza A virus strains, we mutated 14 conserved residues in the PA-C domain that we hypothesized to influence CTD binding (Fig. S6) (11, 13, 26, 27). Only low levels of vRNA, expressed from the transfected plasmid, were observed if the PA subunit was omitted from the transfection (Fig. 4). However, in the presence of a complete wild-type polymerase, we observed mRNA and cRNA, as well as a significant increase in vRNA levels, indicating that the viral polymerase transcribes and replicates the input vRNA. Comparing the RNA levels produced by the wild-type and mutant polymerases, we found that mutations K289A, Y445A, E449A, R454A, and K635A affected transcription with relatively little if any effect on replication. The phenotype of these mutants is fully consistent with CTD binding being required for viral transcription, as this interaction facilitates access of the viral polymerase to capped RNA fragments generated from nascent Pol II transcripts. Other mutations such as L290A, T313A, D419A, L527A,

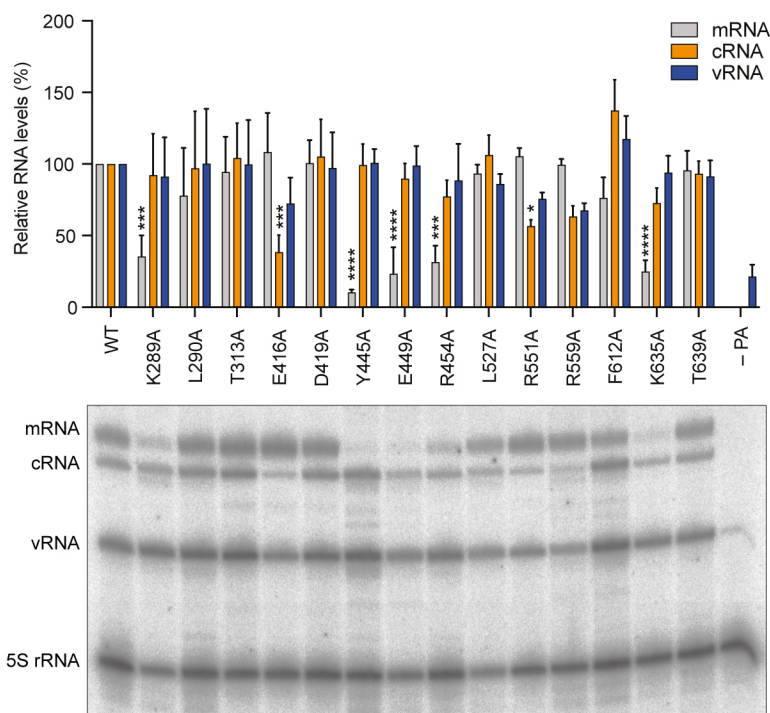


**FIG 4** The effect of mutations in the CTD-binding site of the 1918 pandemic H1N1 influenza A virus polymerase on viral RNA synthesis. HEK 293T cells were transfected to express the 1918 influenza virus polymerase subunits PA (WT and mutant), PB1, and PB2, and nucleoprotein, as well as segment 6 vRNA. For the negative control, the plasmid expressing PA was replaced with an empty vector. Total RNA was isolated 24 h post-transfection and was analyzed by primer extension assay. Top panel, quantification of mRNA, cRNA, and vRNA levels from  $n = 3$  independent vRNP reconstitution assays. Bottom panel, a representative primer extension analysis. 5S rRNA was used as a loading control. The faint bands observed for some of the mutants between the cRNA, vRNA, and 5S rRNA bands are not reproducible between replicates and most likely represent primer extension products from partially degraded RNA. The mean signal intensity is shown relative to the signal intensity from WT 1918 viral polymerase. Data are mean  $\pm$  SEM. Ordinary two-way ANOVA was employed to determine significant differences with \* $P < 0.05$ ; \*\*\* $P < 0.001$ ; and \*\*\*\* $P < 0.0001$ .

R559A, F612A, and T639A had no or only a small effect on transcription indicating that these amino acid residues do not contribute critical interactions to CTD binding. Surprisingly, two mutations, E416A and R551A, specifically reduced cRNA synthesis, suggesting that amino acid residues around the Pol II CTD binding site also participate in the replication of the viral RNA genome.

## DISCUSSION

In this study, we have solved the solution state structure of the 1918 pandemic H1N1 influenza virus polymerase bound to pS5 Pol II CTD using cryo-EM. The structure revealed a continuous density for the CTD peptide with 25 out of the 28 amino acid residues fully resolved. The CTD peptide was found to bind exclusively at the PA-C with two of the phosphorylated serine residues playing prominent roles in guiding the interaction by being accommodated in highly basic grooves. The interaction interface overlaps with that previously observed in a study using polymerase of a bat H17N10 influenza A virus (13). However, in contrast to this study that observed two separate binding sites for the CTD, here we identify a continuous density with the CTD linking the two binding sites. The PB2-C domains remained unstructured in most particles suggesting that binding of CTD in solution does not stabilize the cap-snatching or transcription initiation complexes and that a longer CTD peptide and/or other interacting partners might be required. However, in a small population of particles, the PB2 cap-binding, mid-link, 627, and NLS domains were structured, revealing an arrangement not previously observed. In this novel arrangement, the 627 domain is positioned close to the N-terminus of the CTD peptide providing a potential basic surface for additional interactions with the acidic CTD. Binding of the CTD across PA-C and the adjacent 627 domain could stabilize the 627 domain and, consequently, enable the PB2 cap-binding and PA endonuclease domains to assume a cap-snatching competent conformation. Pol II CTD peptides composed of four heptad repeats used in our study might be too short to cover the entire binding surface that might extend from PA-C across the PB2 627-NLS domains. Further studies using Pol II CTD peptides composed of more than four heptad repeats could reveal further insights into the interaction of the influenza virus polymerase with Pol II CTD.

The Pol II CTD can be phosphorylated at S2, S5, and S7 and on Y1 and T4 of the heptad repeat (16). Binding assays of the influenza A virus polymerase to Pol II CTD peptides containing different phosphorylation patterns revealed a striking preference for pS5 CTD peptides over pS2 or pS7 peptides. Combining pS5 with pS2 or pS7 in various arrangements in the same peptide led to a dramatic reduction of polymerase binding suggesting that the viral polymerase engages with Pol II at a very precise point in the transcription cycle when the capping enzyme is recruited to Pol II (30, 31). Analysis of our structure explains how additional phosphorylation at S2 and S7 would disrupt CTD binding even for peptides that carry phosphorylation at the most critical S5a and S5c positions. Phosphorylation at S2a and S2b would likely be well accommodated as these residues are exposed toward the solvent. On the other hand, phosphorylation at S7a, S7b, S7c, and S2d could be accommodated but would likely require some rearrangement of the peptide. Phosphorylation of S2c would be unlikely to be accommodated given the tight contact with the polymerase and the nearby highly negative charge on S5c. Furthermore, phosphorylation additional to pS5a and pS5c could promote conformational changes in the peptide not compatible with polymerase binding. We observed weak but significant binding to the pS7 peptide. The functional significance of S7 phosphorylation is still poorly understood, but several studies have linked it to events early in the Pol II transcriptional cycle (21). Given the weak binding observed further studies are required, using different methodologies, to assess pS7 peptide binding to the influenza A virus polymerase and its potential functional significance.

We observed that mutations of PA-C at the CTD-binding site cause defects in both transcription and replication. Transcription was affected by mutations in K289A, Y445A, E449A, R454A, and K635A of the PA subunit with little to no effect on genome

replication. These amino acid residues, along with the previously extensively studied R638 (13, 32), are involved in direct interactions with pS5 of the first and third heptad repeat of the Pol II CTD (pS5a and pS5c) as well as Y1 of the first repeat (Y1a), highlighting that interactions with these three amino acids are the most critical for CTD binding. These results are consistent with CTD binding being important for viral mRNA synthesis by enabling cap-snatching. Interestingly, we observed reduced replication of the PA E416A and R551A mutants with little effect on transcription. Recent studies of the influenza C virus polymerase in complex with human and chicken ANP32A revealed that the ANP32A-binding site overlaps with part of the Pol II CTD-binding site (33) (Fig. 5). ANP32 proteins have been shown to be essential factors for the genome replication of all three types of influenza viruses (33–35), and influenza A virus likely also interacts with ANP32A through its PA-C domain. The involvement of influenza A virus PA-C in ANP32A binding is supported by previously published functional data analyzing the effect of mutations in PA-C on ANP32A binding and the replication activity of the viral polymerase (33). We speculate that PA mutations E416A and R551A might also inhibit genome replication through interfering with ANP32A binding. Further structural studies using influenza A virus polymerase in complex with ANP32A could provide further insights into how the alternate binding of Pol II CTD and ANP32A at the same site in PA-C regulate transcription and replication by the viral polymerase. The importance of this site in the viral replication cycle has recently been highlighted through the use of nanobodies (27). Specifically, two nanobodies which bind PA-C at sites adjacent to the CTD peptide binding site and have been shown to block CTD binding, inhibited both mRNA and cRNA synthesis and, consequently, viral growth.

While this study was under review, a new structure of the influenza A virus polymerase bound to a Pol II CTD peptide has been reported (36). Specifically, the structure of the polymerase derived from influenza A/Zhejiang/DTID-ZJU01/2013 (H7N9) virus bound to Pol II CTD has been solved by cryo-EM. The structure reveals a very similar CTD-binding site on PA-C as reported in our study.

In summary, our work has uncovered the structural basis of the binding of the CTD of Pol II to the polymerase of the 1918 pandemic influenza A virus. Future research aiming to understand cap-snatching in molecular detail in the context of mammalian Pol II will require the inclusion of additional accessory proteins suspected to contribute

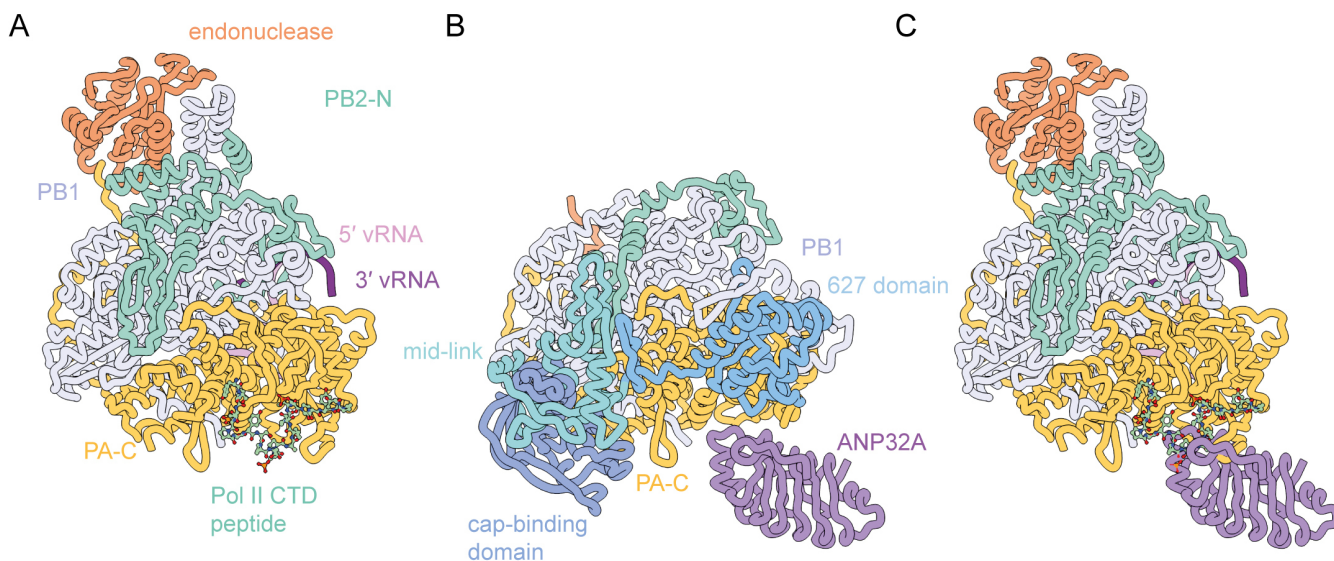


**FIG 5** Comparison of the Pol II CTD and ANP32 binding sites on the PA-C. (A) Influenza A virus polymerase bound to Pol II CTD peptide (PDB ID 8R60). (B) Influenza C virus polymerase in the encapsidating conformation bound to chicken ANP32A (PDB ID 6XZR), aligned on PB1 and PA-C to the structure in panel A. (C) Positioning of the ANP32A structure on the influenza A virus polymerase structure (A) based on the superposition in (B) indicating the overlap of the Pol II CTD and ANP32A-binding sites on PA-C.

to the complex formation between Pol II and the viral polymerase. The highly repetitive and intrinsically disordered nature of the CTD drives phase separation and leads to the recruitment of Pol II and transcription factors that together form condensates (37–41). In the future, CTD-driven phase separation should be investigated within the context of viral infection to facilitate a spatiotemporal understanding of the links between the host transcriptional apparatus and viral transcription and replication beyond the PA-C.

## MATERIALS AND METHODS

### Protein expression and purification

The three polymerase genes from influenza A/Brevig Mission/1/1918 (H1N1) virus were codon optimized for insect cells and synthesized (Synbio Technologies). Genes were then cloned into the Multibac system (42) with protein expression and purification carried out as previously described (43). Cryo-EM studies in this manuscript were carried out using a polymerase that contained a PA D108A endonuclease mutation to reduce RNA degradation. Briefly, Sf9 insect cells were infected with the baculovirus encoding the three viral polymerase genes and harvested 72 h post infection. Cell pellet from one liter of culture was resuspended in 50 mL buffer containing 50 mM HEPES-NaOH, pH 7.5, 500 mM NaCl, 10% vol/vol glycerol, 0.05% wt/vol *n*-octyl beta-D-thioglucopyranoside, 1 mM dithiothreitol which was further supplemented with 1 protease inhibitor cocktail tablet (Roche) and 5 mg RNase A. The cells were lysed with sonication and clarified with centrifugation. The resulting lysate was incubated with IgG Sepharose for 3 h before washing the resin with 50 mM HEPES-NaOH, pH 7.5, 500 mM NaCl, 10% vol/vol glycerol, 0.05% wt/vol *n*-octyl beta-D-thioglucopyranoside, 1 mM dithiothreitol. The protein was eluted by the addition of Tobacco Etch Virus (TEV) protease overnight. The eluted protein was concentrated and applied to a Superdex increase S200 10/300 (GE Healthcare) size exclusion column equilibrated with 25 mM HEPES-NaOH, pH 7.5, 500 mM NaCl, 5% vol/vol glycerol, 0.5 mM dithiothreitol. Fractions containing pure protein were concentrated and stored at –80°C.

### Cryo-EM sample preparation

An aliquot of purified polymerase of the A/Brevig Mission/1/1918 (H1N1) influenza virus with a D108A mutation in the PA subunit was defrosted and viral RNA promoters [5' vRNA 5'-AGUAGAAACAAGGCC-3', 3' vRNA 5'-GGCCUGCUUUUGCUAUU-3' with a 3-nucleotide long extension at the 3' end (*italics*)] were added to a 1.2 molar excess and incubated on ice for 20 min. The sample was then further purified by size exclusion chromatography into a buffer containing 25 mM HEPES-NaOH, pH 7.5, and 500 mM NaCl before being concentrated to 1 mg/mL. A capped RNA primer (5' m7GpppGAAUGCUAUAUAGC), with six complementary bases at the 3' to the 3' vRNA promoter, was added to this sample to a final concentration of 0.2 mM. Additionally, a pS5 Pol II CTD mimic peptide containing four repeats of the heptapeptide consensus sequence (Y<sub>1</sub>S<sub>2</sub>P<sub>3</sub>T<sub>4</sub>pS<sub>5</sub>P<sub>6</sub>S<sub>7</sub>)<sub>4</sub>, with C-terminal amidation, N-terminal biotinylation, and a nine-atom polyethylene glycol spacer between the biotin moiety and the first amino acid (PeptideSynthetics, Peptide Protein Research Ltd) (Table S1), was added to a final concentration of 0.2 mM. Immediately prior to grid preparation, the sample was diluted 1:3 with a buffer containing HEPES-NaOH, pH 7.5, 37.5 mM NaSCN, and 0.0075% (vol/vol) Tween20. A volume of 3.5 μL of the sample was applied to a freshly glow-discharged Quantifoil Holey Carbon R2/1, 200 mesh copper grid which was blotted for 3.5 s and plunge frozen in liquid ethane. All grids were prepared using a Vitrobot mark VI (FEI) at 100% humidity and 20°C.

### Cryo-EM image collection and processing

Data were collected on a 300 kV Titan Krios with a K2 Summit camera (Gatan) and a GIF Quantum energy filter at the Oxford Particle Imaging Centre. Data were collected using

SerialEM (44). Figures were prepared using ChimeraX (45). Data processing is graphically summarized in Fig. S2, and data collection and processing details are presented in Table S2. cryoSPARC V4-4.2 (46, 47) was used to perform patch motion correction, patch CTF estimation, and picking of initial particles using the blob picker. Micrographs with poor pre-processing statistics were manually removed. After 2D classification and generation of an initial high-resolution consensus refinement, these particles were used to train a topaz model (48) and repick particles in the data set. Particles were combined, and duplicates were removed.

After performing rounds of 3D classification on the CTD peptide data set, a consensus refinement involving 303,608 particles resulted in a map with a resolution of 3.22 Å. A model was built into this reconstruction using the 7NHX as a starting model. The model was manually built in COOT before refinement in real space using PHENIX (49). Further 3D classification yielded a reconstruction which contained extra density corresponding to PB2-C. To aid interpretation of the density, the map was modified using deepEM-hancer (50). In this modified map, the previously mentioned model, encompassing the PA, PB1, and N-terminal region of PB2 (PB2-N) subunits, was positioned. Subsequently, the PB2-C domains (extracted from PDB 7NHX) were placed into the corresponding density. Due to the low resolution of the density in this region, the domains were manually connected in COOT before restrained rigid-body real-space and ADP refinement.

## Cells and plasmids

Human embryonic kidney (HEK) 293T cells (293T) were grown in Dulbecco's modified Eagle's medium (DMEM, Gibco) supplemented with 10% fetal bovine serum (FBS, Gibco) and cultured at 37°C with 5% CO<sub>2</sub>. The pCAGGS-PA-1918, pCAGGS-PB1-1918, pCAGGS-PB2-1918, pCAGGS-NP-1918 plasmids expressing the vRNP components of influenza A/Brevig Mission/1/1918 virus, have been described previously (51). The pPOLI-NA-RT plasmid expressing a segment 6 vRNA template under the control of a human RNA polymerase I (Pol I) has also been described (52). Mutations in pCAGGS-PA-1918 were introduced using site-directed mutagenesis. All constructs were confirmed by Sanger sequencing.

## vRNP reconstitution assay, RNA isolation, and analysis

To compare the activity of mutant viral polymerases in cell culture, HEK 293T cells were grown to 80% confluency in six-well dishes and transfected with 0.5 µg of each of wild-type (WT) or mutant pCAGGS-PA-1918, pCAGGS-PB1-1918, pCAGGS-PB2-1918, pCAGGS-NP-1918, and pPOLI-NA-RT plasmids. For the negative control, pCAGGS-PA-1918 was replaced with an empty vector. Transfections were performed using Lipofectamine 2000 (Invitrogen) according to the manufacturer's instructions. Total RNA from transfected cells was extracted using TRI reagent (Sigma) according to the manufacturer's instructions 24 h post transfection. Levels of mRNA, cRNA, and vRNA were analyzed by primer extension assay as previously described (53). In brief, extracted RNA was reverse transcribed by SuperScript III reverse transcriptase (Invitrogen) and <sup>32</sup>P-labeled NA-specific primers along with a primer targeting endogenous 5S rRNA as an internal control. Primer extension products were separated by 6% denaturing PAGE with 7 M urea in TBE buffer, and bands were detected by phosphorimaging on an FLA-5000 scanner (Fuji). The cDNA was analyzed using ImageJ (Fiji) and Prism 8 (GraphPad).

## Immunoblotting

Immunoblotting was performed to determine expression levels of WT and mutant PA in HEK293T cells. PA, NP (transfection control), and GAPDH (loading control) were probed overnight at 4°C with rabbit anti-PA (6) (1:500), rabbit anti-NP (1:5,000) (Genetex), and rabbit anti-GAPDH (1:1,000) (Cell Signalling Technology). Goat anti-rabbit antibody conjugated to horseradish peroxidase (HRP) was used as secondary antibody (1:10,000)

(Genetex). Bands were detected using Amersham ECL Western blotting detection reagents (GE Healthcare).

### Design and synthesis of Pol II CTD mimic peptides

Peptides were chemically synthesized by solid-phase peptide synthesis (Peptide Protein Research Ltd.). The designed peptides contain four repeats of the heptapeptide consensus sequence of the Pol II CTD (YSPTSPS) with modifications to mimic different phosphorylation states of serine residues at position 2, position 5, and position 7 of the CTD. Full amino acid sequences are detailed in Table S1. All peptides were synthesized with C-terminal amidation and N-terminal biotinylation and included a nine-atom polyethylene glycol spacer between the biotin moiety and the first amino acid. Peptides were purified by high-performance liquid chromatography to at least 90% purity, and peptide quality was confirmed by mass spectrometry.

### Binding assay of influenza virus polymerase to Pol II CTD

The binding of purified viral polymerase to synthetic four-heptad repeat Pol II CTD mimic peptides (Table S1) was performed as previously described (22, 27). In brief, biotinylated Pol II CTD mimic peptide (20 µg) was immobilized on 10 µL streptavidin agarose resin (Thermo Scientific) for 2 h at 4 °C in binding buffer [10 mM HEPES (PAA catalog no. S11-001), 150 mM NaCl, 0.1% (vol/vol) Igepal, 1 × Halt protease inhibitor cocktail (Pierce), 1% (wt/vol) bovine serum albumin (BSA)], followed by washing with wash buffer [10 mM HEPES (PAA catalog no. S11-001), 150 mM NaCl, 0.1% (vol/vol) Igepal, 1 mM PMSF]. After washing the beads with wash buffer, 4 µg of 1918 influenza virus polymerase in binding buffer was incubated with the peptide-bound beads for 2 h at 4 °C. Beads were washed and boiled in SDS-PAGE sample buffer at 95 °C for 5 min, followed by SDS-PAGE analysis and silver staining to visualize protein bands according to the manufacturer's instructions (Invitrogen). Quantitation of bands was performed using ImageJ.

### ACKNOWLEDGMENTS

We thank Haitian Fan and Jane Sharps for their assistance with protein expression and advice on the functional assays. We also thank members of the Grimes and Fodor laboratories for helpful comments and discussions.

This work was supported by Wellcome Investigator Awards 200835/Z/16/Z and 222510/Z/21/Z (to J.M.G.); Medical Research Council (MRC) program grants MR/R009945/1 and MR/X008312/1 (to E.F.); Ministry of Education, Youth, and Sports of the Czech Republic CZ.02.01.01/00/22\_008/0004575 (to R.S.); and Biotechnology and Biological Sciences Research Council (BBSRC) Oxford Interdisciplinary Bioscience Doctoral Training Partnership training grant BB/M011224/1 (to A.B.). Access to electron microscopes was provided by the OPIC Electron Microscopy Facility [funded by Wellcome JIF (060208/Z/00/Z) and equipment (093305/Z/10/Z) grants]. Access to computational resources was supported by the Wellcome Trust Core Award Grant Number 203141/Z/16/Z with additional support from the NIHR Oxford BRC. The views expressed are those of the author(s) and not necessarily those of the NHS, the NIHR, or the Department of Health. For the purpose of Open Access, the authors have applied a CC BY public copyright licence to any Author Accepted Manuscript version arising from this submission.

### AUTHOR AFFILIATIONS

<sup>1</sup>Division of Structural Biology, Centre for Human Genetics, University of Oxford, Oxford, United Kingdom

<sup>2</sup>Sir William Dunn School of Pathology, University of Oxford, Oxford, United Kingdom

<sup>3</sup>CEITEC—Central European Institute of Technology, Masaryk University, Brno, Czechia

<sup>4</sup>National Centre for Biomolecular Research, Faculty of Science, Masaryk University, Brno, Czechia

## PRESENT ADDRESS

Jeremy Keown, School of Life Sciences, University of Warwick, Coventry, United Kingdom

## AUTHOR ORCID*s*

Jeremy Keown  <http://orcid.org/0000-0003-0159-9257>

Alaa Baazaoui  <http://orcid.org/0009-0001-7975-482X>

Ervin Fodor  <http://orcid.org/0000-0003-3249-196X>

Jonathan M. Grimes  <http://orcid.org/0000-0001-9698-0389>

## FUNDING

Funder	Grant(s)	Author(s)
<a href="#">Wellcome Trust (WT)</a>	200835/Z/16/Z, 222510/Z/21/Z, 060208/Z/00/Z, 093305/Z/10/Z, 203141/Z/16/Z	Jonathan M. Grimes
<a href="#">UKRI   Medical Research Council (MRC)</a>	MR/R009945/1, MR/X008312/1	Ervin Fodor
<a href="#">Ministry of education, youth and sports of the Czech Republic</a>	CZ.02.01.01/00/22_008/0004575	Richard Štefl
<a href="#">UKRI   Biotechnology and Biological Sciences Research Council (BBSRC)</a>	BB/M011224/1	Alaa Baazaoui

## DATA AVAILABILITY

Map and models have been deposited in the Electron Microscopy and Protein Data Bank, respectively. The structure of the 1918 pandemic influenza A virus polymerase bound to vRNA and Pol II CTD peptide is deposited under [EMD-18945](#) and [PDB-8R60](#), the structure of the 1918 pandemic influenza A virus polymerase bound to vRNA and Pol II CTD peptide with ordered PB2 is deposited under [EMD-18947](#) and [PDB-8R65](#). Source data as well as plasmids are available upon request.

## ADDITIONAL FILES

The following material is available [online](#).

### Supplemental Material

**Supplemental tables and figures (JVI00138-24-s0001.pdf).** Tables S1 and S2; Figures S1 to S6.

## REFERENCES

- Eisfeld AJ, Neumann G, Kawaoka Y. 2015. At the centre: influenza A virus ribonucleoproteins. *Nat Rev Microbiol* 13:28–41. <https://doi.org/10.1038/nrmicro3367>
- Te Velthuis AJW, Fodor E. 2016. Influenza virus RNA polymerase: insights into the mechanisms of viral RNA synthesis. *Nat Rev Microbiol* 14:479–493. <https://doi.org/10.1038/nrmicro.2016.87>
- Zhu Z, Fodor E, Keown JR. 2023. A structural understanding of influenza virus genome replication. *Trends Microbiol* 31:308–319. <https://doi.org/10.1016/j.tim.2022.09.015>
- Walker AP, Fodor E. 2019. Interplay between influenza virus and the host RNA polymerase II transcriptional machinery. *Trends Microbiol* 27:398–407. <https://doi.org/10.1016/j.tim.2018.12.013>
- Wandzik JM, Kouba T, Cusack S. 2021. Structure and function of influenza polymerase. *Cold Spring Harb Perspect Med* 11:a038372. <https://doi.org/10.1101/cshperspect.a038372>
- Engelhardt OG, Smith M, Fodor E. 2005. Association of the influenza A virus RNA-dependent RNA polymerase with cellular RNA polymerase II. *J Virol* 79:5812–5818. <https://doi.org/10.1128/JVI.79.9.5812-5818.2005>
- Vreede FT, Chan AY, Sharps J, Fodor E. 2010. Mechanisms and functional implications of the degradation of host RNA polymerase II in influenza virus infected cells. *Virology* 396:125–134. <https://doi.org/10.1016/j.virol.2009.10.003>
- Bauer DLV, Tellier M, Martínez-Alonso M, Nojima T, Proudfoot NJ, Murphy S, Fodor E. 2018. Influenza virus mounts a two-pronged attack

- on host RNA polymerase II transcription. *Cell Rep* 23:2119–2129. <https://doi.org/10.1016/j.celrep.2018.04.047>
9. Rodriguez A, Pérez-González A, Nieto A. 2007. Influenza virus infection causes specific degradation of the largest subunit of cellular RNA polymerase II. *J Virol* 81:5315–5324. <https://doi.org/10.1128/JVI.02129-06>
  10. Krischuns T, Lukarska M, Naffakh N, Cusack S. 2021. Influenza virus RNA-dependent RNA polymerase and the host transcriptional apparatus. *Annu Rev Biochem* 90:321–348. <https://doi.org/10.1146/annurev-biochem-072820-100645>
  11. Krischuns T, Isel C, Drncova P, Lukarska M, Pflug A, Paisant S, Navratil V, Cusack S, Naffakh N. 2022. Type B and type A influenza polymerases have evolved distinct binding interfaces to recruit the RNA polymerase II CTD. *PLoS Pathog* 18:e1010328. <https://doi.org/10.1371/journal.ppat.1010328>
  12. Serna Martin I, Hengrung N, Renner M, Sharps J, Martínez-Alonso M, Masiulis S, Grimes JM, Fodor E. 2018. A mechanism for the activation of the influenza virus transcriptase. *Molecular Cell* 70:1101–1110. <https://doi.org/10.1016/j.molcel.2018.05.011>
  13. Lukarska M, Fournier G, Pflug A, Resa-Infante P, Reich S, Naffakh N, Cusack S. 2017. Structural basis of an essential interaction between influenza polymerase and Pol II CTD. *Nature* 541:117–121. <https://doi.org/10.1038/nature20594>
  14. Morel J, Sedano L, Lejal N, Da Costa B, Batsché E, Muchardt C, Delmas B. 2022. The influenza virus RNA-polymerase and the host RNA-polymerase II: RPB4 is targeted by a PB2 domain that is involved in viral transcription. *Viruses* 14:518. <https://doi.org/10.3390/v14030518>
  15. Dieci G. 2021. Removing quote marks from the RNA polymerase II CTD 'code'. *Biosystems* 207:104468. <https://doi.org/10.1016/j.biosystems.2021.104468>
  16. Zaborowska J, Egloff S, Murphy S. 2016. The Pol II CTD: new twists in the tail. *Nat Struct Mol Biol* 23:771–777. <https://doi.org/10.1038/nsmb.3285>
  17. Jasnovidova O, Stefl R. 2013. The CTD code of RNA polymerase II: a structural view. *Wiley Interdiscip Rev RNA* 4:1–16. <https://doi.org/10.1002/wrna.1138>
  18. Yurko NM, Manley JL. 2018. "The RNA polymerase II CTD "orphan" residues: emerging insights into the functions of Tyr-1, Thr-4, and Ser-7". *Transcription* 9:30–40. <https://doi.org/10.1080/21541264.2017.1338176>
  19. Schüller R, Forné I, Straub T, Schrieck A, Texier Y, Shah N, Decker T-M, Cramer P, Imhof A, Eick D. 2016. Heptad-specific phosphorylation of RNA polymerase II CTD. *Mol Cell* 61:305–314. <https://doi.org/10.1016/j.molcel.2015.12.003>
  20. Suh H, Ficarro SB, Kang UB, Chun Y, Marto JA, Buratowski S. 2016. Direct analysis of phosphorylation sites on the Rpb1 C-terminal domain of RNA polymerase II. *Mol Cell* 61:297–304. <https://doi.org/10.1016/j.molcel.2015.12.021>
  21. Lyons DE, McMahon S, Ott M. 2020. A combinatorial view of old and new RNA polymerase II modifications. *Transcription* 11:66–82. <https://doi.org/10.1080/21541264.2020.1762468>
  22. Martínez-Alonso M, Hengrung N, Fodor E. 2016. RNA-free and ribonucleoprotein-associated influenza virus polymerases directly bind the serine-5-phosphorylated carboxyl-terminal domain of host RNA polymerase II. *J Virol* 90:6014–6021. <https://doi.org/10.1128/JVI.00494-16>
  23. Whelan M, Pelchat M. 2022. Role of RNA polymerase II promoter-proximal pausing in viral transcription. *Viruses* 14:2029. <https://doi.org/10.3390/v14092029>
  24. Pflug A, Guilligay D, Reich S, Cusack S. 2014. Structure of influenza A polymerase bound to the viral RNA promoter. *Nature* 516:355–360. <https://doi.org/10.1038/nature14008>
  25. Wandzick JM, Kouba T, Karuppasamy M, Pflug A, Drncova P, Provaznik J, Azevedo N, Cusack S. 2020. A structure-based model for the complete transcription cycle of influenza polymerase. *Cell* 181:877–893. <https://doi.org/10.1016/j.cell.2020.03.061>
  26. Fan H, Walker AP, Carrique L, Keown JR, Serna Martin I, Karia D, Sharps J, Hengrung N, Pardon E, Steyaert J, Grimes JM, Fodor E. 2019. Structures of influenza A virus RNA polymerase offer insight into viral genome replication. *Nature* 573:287–290. <https://doi.org/10.1038/s41586-019-1530-7>
  27. Keown JR, Zhu Z, Carrique L, Fan H, Walker AP, Serna Martin I, Pardon E, Steyaert J, Fodor E, Grimes JM. 2022. Mapping inhibitory sites on the RNA polymerase of the 1918 pandemic influenza virus using nanobodies. *Nat Commun* 13:251. <https://doi.org/10.1038/s41467-021-27950-w>
  28. Li H, Wu Y, Li M, Guo L, Gao Y, Wang Q, Zhang J, Lai Z, Zhang X, Zhu L, Lan P, Rao Z, Liu Y, Liang H. 2023. An intermediate state allows influenza polymerase to switch smoothly between transcription and replication cycles. *Nat Struct Mol Biol* 30:1183–1192. <https://doi.org/10.1038/s41594-023-01043-2>
  29. te Velthuis AJW, Grimes JM, Fodor E. 2021. Structural insights into RNA polymerases of negative-sense RNA viruses. *Nat Rev Microbiol* 19:303–318. <https://doi.org/10.1038/s41579-020-00501-8>
  30. Heidemann M, Hintermair C, Voß K, Eick D. 2013. Dynamic phosphorylation patterns of RNA polymerase II CTD during transcription. *Biochim Biophys Acta* 1829:55–62. <https://doi.org/10.1016/j.bbaggm.2012.08.013>
  31. Core L, Adelman K. 2019. Promoter-proximal pausing of RNA polymerase II: a nexus of gene regulation. *Genes Dev* 33:960–982. <https://doi.org/10.1101/gad.325142.119>
  32. Fodor E, Mingay LJ, Crow M, Deng T, Brownlee GG. 2003. A single amino acid mutation in the PA subunit of the influenza virus RNA polymerase promotes the generation of defective interfering RNAs. *J Virol* 77:5017–5020. <https://doi.org/10.1128/jvi.77.8.5017-5020.2003>
  33. Carrique L, Fan H, Walker AP, Keown JR, Sharps J, Staller E, Barclay WS, Fodor E, Grimes JM. 2020. Host ANP32A mediates the assembly of the influenza virus replicase. *Nature* 587:638–643. <https://doi.org/10.1038/s41586-020-2927-z>
  34. Staller E, Sheppard CM, Neasham PJ, Mistry B, Peacock TP, Goldhill DH, Long JS, Barclay WS. 2019. ANP32 proteins are essential for influenza virus replication in human cells. *J Virol* 93:e00217-19. <https://doi.org/10.1128/JVI.00217-19>
  35. Zhang H, Zhang Z, Wang Y, Wang M, Wang X, Zhang X, Ji S, Du C, Chen H, Wang X. 2019. Fundamental contribution and host range determination of ANP32A and ANP32B in influenza A virus polymerase activity. *J Virol* 93:e00174-19. <https://doi.org/10.1128/JVI.00174-19>
  36. Krischuns T, Arragain B, Isel C, Paisant S, Budt M, Wolff T, Cusack S, Naffakh N. 2024. The host RNA polymerase II C-terminal domain is the anchor for replication of the influenza virus genome. *Nat Commun* 15:1064. <https://doi.org/10.1038/s41467-024-45205-2>
  37. Boehning M, Dugast-Darzacq C, Rankovic M, Hansen AS, Yu T, Marie-Nelly H, McSwiggen DT, Kokic G, Dailey GM, Cramer P, Darzacq X, Zweckstetter M. 2018. RNA polymerase II clustering through carboxy-terminal domain phase separation. *Nat Struct Mol Biol* 25:833–840. <https://doi.org/10.1038/s41594-018-0112-y>
  38. Flores-Solis D, Lushpinskaia IP, Polyansky AA, Changiarath A, Boehning M, Mirkovic M, Walshe J, Pietrek LM, Cramer P, Stelzl LS, Zagrovic B, Zweckstetter M. 2023. Driving forces behind phase separation of the carboxy-terminal domain of RNA polymerase II. *Nat Commun* 14:5979. <https://doi.org/10.1038/s41467-023-41633-8>
  39. Cho WK, Spille JH, Hecht M, Lee C, Li C, Grube V, Cisse II. 2018. Mediator and RNA polymerase II clusters associate in transcription-dependent condensates. *Science* 361:412–415. <https://doi.org/10.1126/science.aar4199>
  40. Guo YE, Manteiga JC, Henninger JE, Sabari BR, Dall'Agnese A, Hannett NM, Spille J-H, Afeyan LK, Zamudio AV, Shrinivas K, Abraham BJ, Boija A, Decker T-M, Rimel JK, Fant CB, Lee TI, Cisse II, Sharp PA, Taatjes DJ, Young RA. 2019. Pol II phosphorylation regulates a switch between transcriptional and splicing condensates. *Nature* 572:543–548. <https://doi.org/10.1038/s41586-019-1464-0>
  41. Sabari BR, Dall'Agnese A, Boija A, Klein IA, Coffey EL, Shrinivas K, Abraham BJ, Hannett NM, Zamudio AV, Manteiga JC, Li CH, Guo YE, Day DS, Schuijers J, Vasile E, Malik S, Hnisz D, Lee TI, Cisse II, Roeder RG, Sharp PA, Chakraborty AK, Young RA. 2018. Coactivator condensation at super-enhancers links phase separation and gene control. *Science* 361. <https://doi.org/10.1126/science.aar3958>
  42. Bieniossek C, Imasaki T, Takagi Y, Berger I. 2012. MultiBac: expanding the research toolbox for multiprotein complexes. *Trends Biochem Sci* 37:49–57. <https://doi.org/10.1016/j.tibs.2011.10.005>
  43. York A, Hengrung N, Vreede FT, Huiskonen JT, Fodor E. 2013. Isolation and characterization of the positive-sense replicative intermediate of a negative-strand RNA virus. *Proc Natl Acad Sci U S A* 110:E4238–45. <https://doi.org/10.1073/pnas.1315068110>
  44. Mastrorarde DN. 2003. Serialec: a program for automated tilt series acquisition on tecai microscopes using prediction of specimen

- position. *Microsc Microanal* 9:1182–1183. <https://doi.org/10.1017/S1431927603445911>
45. Pettersen EF, Goddard TD, Huang CC, Meng EC, Couch GS, Croll TI, Morris JH, Ferrin TE. 2021. UCSF chimeraX: structure visualization for researchers, educators, and developers. *Protein Sci* 30:70–82. <https://doi.org/10.1002/pro.3943>
46. Punjani A, Rubinstein JL, Fleet DJ, Brubaker MA. 2017. cryoSPARC: algorithms for rapid unsupervised cryo-EM structure determination. *Nat Methods* 14:290–296. <https://doi.org/10.1038/nmeth.4169>
47. Punjani A, Zhang H, Fleet DJ. 2020. Non-uniform refinement: adaptive regularization improves single-particle cryo-EM reconstruction. *Nat Methods* 17:1214–1221. <https://doi.org/10.1038/s41592-020-00990-8>
48. Bepler T, Morin A, Rapp M, Brasch J, Shapiro L, Noble AJ, Berger B. 2019. Positive-unlabeled convolutional neural networks for particle picking in cryo-electron micrographs. *Nat Methods* 16:1153–1160. <https://doi.org/10.1038/s41592-019-0575-8>
49. Afonine PV, Poon BK, Read RJ, Sobolev OV, Terwilliger TC, Urzhumtsev A, Adams PD. 2018. Real-space refinement in PHENIX for cryo-EM and crystallography. *Acta Crystallogr D Struct Biol* 74:531–544. <https://doi.org/10.1107/S2059798318006551>
50. Sanchez-Garcia R, Gomez-Blanco J, Cuervo A, Carazo JM, Sorzano COS, Vargas J. 2021. Deepemhancer: a deep learning solution for cryo-EM volume post-processing. *Commun Biol* 4:874. <https://doi.org/10.1038/s42003-021-02399-1>
51. Tumpey TM, Basler CF, Aguilar PV, Zeng H, Solórzano A, Swayne DE, Cox NJ, Katz JM, Taubenberger JK, Palese P, García-Sastre A. 2005. Characterization of the reconstructed 1918 spanish influenza pandemic virus. *Science* 310:77–80. <https://doi.org/10.1126/science.1119392>
52. Fodor E, Devenish L, Engelhardt OG, Palese P, Brownlee GG, García-Sastre A. 1999. Rescue of influenza A virus from recombinant DNA. *J Virol* 73:9679–9682. <https://doi.org/10.1128/JVI.73.11.9679-9682.1999>
53. te Velthuis AJW, Robb NC, Kapanidis AN, Fodor E. 2016. The role of the priming loop in influenza A virus RNA synthesis. *Nat Microbiol* 1:16029. <https://doi.org/10.1038/nmicrobiol.2016.29>